The Amplify-and-Forward Cooperative Uplink Using Multiple-Symbol Differential Sphere-Detection

Li Wang and Lajos Hanzo

School of ECS, University of Southampton, SO17 1BJ, UK.

Tel: +44-23-8059 3125, Fax: +44-23-8059 4508

Email: {lw05r, lh}@ecs.soton.ac.uk; http://www-mobile.ecs.soton.ac.uk

Abstract

It is widely recognized that the differential amplify-and-forward (DAF) transmission scheme is capable of providing a superior performance compared to classic direct transmissions employing differential detection in slow-fading channels and in fact it may even outperform coherent detection aided systems relying on realistic imperfect channel estimates. However, in reality the channels connecting the multiple nodes of a cooperative system typically become time-selective due to the relative mobility of the cooperating terminals. Hence, the performance gain achieved may erode as the environment becomes more time-selective. Hence in this paper, we specifically design the multiple-symbol based differential sphere detection (MSDSD) for the DAF-aided cooperative system, which is capable of achieving a significant performance gain for transmission over time-selective channels.

I. INTRODUCTION

Multiple antenna aided diversity techniques [1] constitute powerful arrangements of mitigating the deleterious effects of fading, hence improving the end-to-end system performance, which is usually achieved by multiple co-located antenna elements at the transmitter and/or receiver. However, it is often impractical for the mobile to

Acknowledgements: The work reported in this paper has formed part of the Core 4 Research Programme of the Virtual Centre of Excellence in Mobile and Personal Communications, Mobile VCE, www.mobilevce.com, whose funding support, including that of EPSRC, is gratefully acknowledged.

employ a large number of antennas for the sake of achieving a diversity gain due to its limited size. Furthermore, owing to the limited separation of the antenna elements, they rarely experience independent fading, which limits the achievable diversity gain and may be further compromised by the detrimental effects of the shadow fading, imposing further signal correlation amongst the antennas in each other's vicinity. Fortunately, in multi-user wireless systems cooperating mobiles may share their antennas in order to achieve uplink transmit diversity by formig a *virtual antenna array* (VAA) in a distributed fashion. Thus, so-called cooperative diversity relying on the cooperation among multiple terminals may be achieved [2, 3].

On the other hand, in order to carry out classic coherent detection, channel estimation is required at the receiver, which relies on using training pilot signals and exploits the fact that in general, the consecutive channel impulse response (CIR) taps are correlated in time as governed by the vehicular speed, i.e. the Doppler frequency. However, channel estimation for an M-transmitter, N-receiver MIMO system requires the estimation of $(M \times N)$ CIRs, which may impose both an excessive complexity and a high pilot overhead, especially in mobile environments associated with relatively rapidly fluctuating channel conditions. Therefore, in such situations, differntially encoded transmissions combined with non-coherent detection requiring no channel state information (CSI) at the receiver becomes an attractive design alternative, leading to differential modulation assisted cooperative communications [4].

It is widely recognized at low mobile velocities that DAF-aided cooperative transmission [4] is capable of outperforming classic direct transmission using coherent detection. However, the performance of the former scheme rapidly degrades, as the channel connecting the multiple terminals becomes more time-selective and/or dispersive. Recently, in order to mitigate the error floor encountered by differentially encoded direct transmission combined with conventional differential detection (CDD) employing an *observation window size* of $N_{wind} = 2$, a multiple-symbol based differential sphere detection (MSDSD) technique using $N_{wind} > 2$ has been proposed in [5, 6]. In the light of the above observations, in this paper we specifically design the MSDSD scheme for the DAF-aided cooperative cellular uplink, improving its robustness to time-selective propagation environments induced by the relatively high-speed mobility among multiple cooperating users.

II. System Model

Now we consider a U-user cooperation-aided system, where signal transmission involves two transmission phases, namely, the broadcast phase-I and the relay phase-II. In both phases, any of the well-established multiple access scheme can be employed by the users to guarantee orthogonal transmission among them. In this paper, TDMA is

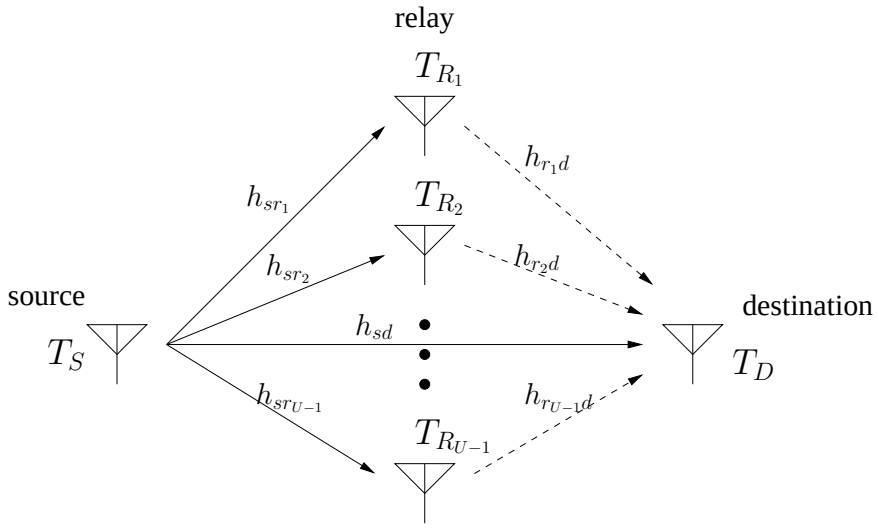

Fig. 1. Multiple-Relay-Node-Aided Cooperative Communication Scheme.

considered for the sake of simplicity. Furthermore, due to the symmetry of channel allocation among users, we focus our attention on the information transmission of the source terminal T_S seen in Fig. 1, which potentially employs $(U-1)$ relay terminals $T_{R_1}, T_{R_2}, \cdots, T_{R_{U-1}}$ in order to achieve cooperative diversity by forming a VAA. Without loss of generality, we simply assume the employment of a single antenna for each terminal, and a unity total power P shared by the collaborating mobiles for transmitting a symbol, namely, $\sum_{u=1}^{U-1} P_{r_u} = 1 - P_s$, where P_s and P_{r_u} represent the power consumed by the source node and the uth relay node, respectively.

In order to avoid channel estimation in the user-cooperation-aided systems considered, the source node differentially encodes its information symbols $v_{sd}[n] \in \mathcal{M}_c = \{e^{j2\pi m/M}; m = 0, 1, \cdots, M-1\}$, each of which contains $\log_2 M$-bit information, as: $s_{sd}[n] = s_{sd}[n-1]v_{sd}[n]$. For the sake of mitigating the impairments imposed by the time-selective channels on the differential transmission, frame-based rather than symbol-based user-cooperation is carried out, which is achieved at the expense of both a higher detection delay and increased memory requirements. Hence, the source continuously broadcasts L_f differentially encoded DPSK signals $s_{sd}[n],\ (n = 0, 1, \cdots, L_f - 1)$ during phase-I, while the destination as well as the relay terminals receive and store them. In the ensuing phase-II, the DAF scheme [4] is employed by the relay node. Specifically, the amplifed signal transmitted by the uth relay

$$\mathbf{S}_n = \mathrm{diag}\{\underbrace{s_{sd}[n], \cdots, s_{sd}[n]}_{U\ elements}\} = \mathrm{diag}\{\underbrace{\mathrm{e}^{j2\pi m/M}, \cdots, \mathrm{e}^{j2\pi m/M}}_{U\ elements}\} \tag{4}$$

$$\mathbf{H}_n = \Big[\sqrt{P_S}h_{sd}[n],\ \sqrt{P_S}f_{AM_{r_1}}h_{sr_1}[n]h_{r_1d}[n+1\cdot L_f], \cdots, \sqrt{P_S}f_{AM_{r_{U-1}}}h_{sr_{U-1}}[n]h_{r_{U-1}d}[n+(U-1)\cdot L_f]\Big]^T \tag{5}$$

where $m = 0, 1, \cdots, M-1$.

$$\mathbf{W}_n = \Big[w_{sd}[n],\ f_{AM_{r_1}}w_{sr_1}[n]h_{r_1d}[n+1\cdot L_f]+w_{r_1d}[n+1\cdot L_f],\ \cdots, f_{AM_{r_{U-1}}}w_{sr_{U-1}}[n]h_{r_{U-1}d}[n+(U-1)\cdot L_f]+w_{r_{U-1}d}[n+(U-1)\cdot L_f]\Big]^T \tag{6}$$

node can be expressed as:

$$s_{r_ud}[n+uL_f] = f_{AM_{r_u}}y_{sr_u}[n], \tag{1}$$

$$= f_{AM_{r_u}}(\sqrt{P_s}s_{sd}[n]h_{sr_u}[n]+w_{sr_u}[n]), \tag{2}$$

where $y_{sr_u}[n]$ is the received signal at the uth relay node and $f_{AM_{r_u}}$ is the gain provided by the uth relay node in order to ensure that the average transmit power of the uth relay node becomes P_{r_u}, which is given in [4] as $f_{AM_{r_u}} = \sqrt{\frac{P_{r_u}}{P_s\sigma^2_{sr_u}+N_0}}$, with $\sigma^2_{sr_u}$ and N_0 being the variance of the channel's envelope between the source and the uth relay node and the noise variance, respectively. We now construct a *single-symbol system model* for the souce node's nth transmitted symbol in the context of the TDMA-based user-cooperation aided system of Fig. 1 as:

$$\mathbf{Y}_n = \mathbf{S}_n\mathbf{H}_n + \mathbf{W}_n, \tag{3}$$

where $\mathbf{S}_n$, $\mathbf{H}_n$ and $\mathbf{W}_n$, respectively, are given by (4), (5) and (6) at the top of the next page, which represent the *equivalent transmitted user-cooperation signal matrix*, the *equivalent channel matrix* and the *equivalent noise matrix*, respectively. The former one has $(U \times U)$ elements, while both of the latter two have $(U \times N_r)$ elements, where N_r is the number of receive antennas.

Then, based on (4), (5) and (6), we can also construct the *equivalent multiple-symbol system model* as:

$$\underline{\mathbf{Y}} = \underline{\mathbf{S}_d}\underline{\mathbf{H}} + \underline{\mathbf{W}}, \tag{7}$$

where the received signal block matrix $\underline{\mathbf{Y}}$, which contains N_{wind} user-cooperation based received symbols corresponding to N_{wind} consecutively transmitted differentially encoded symbols $s_{sd}[n], (n = 0, 1, \cdots, N_{wind}-1)$ by the source node, namely: $\underline{\mathbf{Y}} = [\mathbf{Y}_n^T\ \mathbf{Y}_{n+1}^T\ \cdots\ \mathbf{Y}_{n+N_{wind}-1}^T]^T$, and the channel's block matrix $\underline{\mathbf{H}}$ as well as the AWGN block matrix $\underline{\mathbf{W}}$ are defined likewise as $\underline{\mathbf{H}} = [\mathbf{H}_n^T\ \mathbf{H}_{n+1}^T\ \cdots\ \mathbf{H}_{n+N_{wind}-1}^T]^T$, and $\underline{\mathbf{W}} = [\mathbf{W}_n^T\ \mathbf{W}_{n+1}^T\ \cdots\ \mathbf{W}_{n+N_{wind}-1}^T]^T$, respectively. Moreover, the diagonal block matrix of the transmitted signal is constructed as $\underline{\mathbf{S}_d} = diag\{\mathbf{S}_n,\ \mathbf{S}_{n+1},\ \cdots,\ \mathbf{S}_{n+N_{wind}-1}\}$.

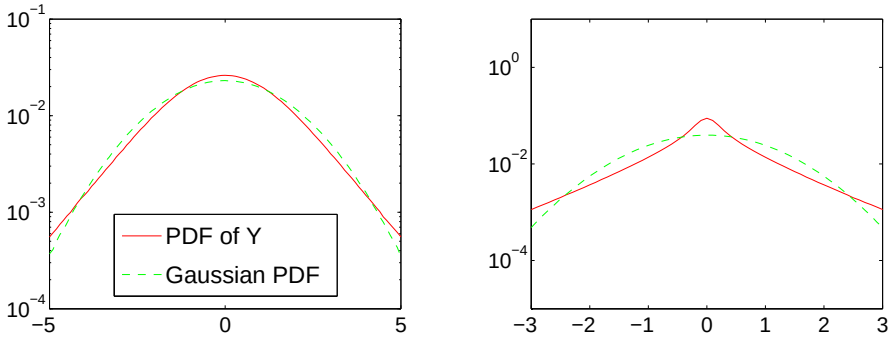

(a) SNR=0 dB (b) SNR=20 dB

Fig. 2. PDF of the received signal $\underline{\mathbf{Y}}$ in (7).

III. Mutiple-Symbol Differential Sphere Detection Design for DAF-Aided Cooperative Transmissions

A. Principle of Multiple-Symbol Differential Detection

We note that most terms in $\mathbf{W}_n$ and $\mathbf{H}_n$ of (5) and (6) do not exhibit a standard Gaussian distribution. However, our informal simulation-based investigations suggest that the resultant noise processes are near-Gaussian distributed. As a result, the probability density function (PDF) of the received signal in (7) is also near-Gaussian especially for low SNRs, as seen in Fig. (2). Hence, under the simplifying assumption that the *equivalent* fading and noise are zero-mean complex Gaussian processes, the PDF of the non-coherent receiver's output $\underline{\mathbf{Y}}$ can be approximately obtained based on its counterpart derived for the single-transmit-antenna scenario [7] as:

$$Pr(\underline{\mathbf{Y}}|\underline{\mathbf{S}}_d) \approx \frac{\exp(-Tr\{\underline{\mathbf{Y}}^H \underline{\Psi}^{-1} \underline{\mathbf{Y}})}{(\pi^{UN_{wind}} \det(\underline{\Psi}))^{N_r}}, \tag{8}$$

where the conditional autocorrelation matrix is given by:

$$\underline{\Psi} = \mathcal{E}\{\underline{\mathbf{Y}}\underline{\mathbf{Y}}^H|\underline{\mathbf{S}}_d\}, \tag{9}$$

$$= \underline{\mathbf{S}}_d \mathcal{E}\{\underline{\mathbf{H}}\underline{\mathbf{H}}^H\} \underline{\mathbf{S}}_d{}^H + \mathcal{E}\{\underline{\mathbf{W}}\underline{\mathbf{W}}^H\}. \tag{10}$$

Note that we consider Rayleigh fading having an autocorrelation function of $\varphi^t[\kappa] \triangleq \mathcal{E}\{h[n+\kappa]h^*[n]\} = J_0(2\pi f_d \kappa)$ according to the widely-used Clarke model, where $J_0(\cdot)$ and f_d represent the zero-order Bessel function of first kind and the normalized Doppler frequency, respectively. Thus, in the context of the DAF-aided user-cooperation system of Fig. 1, the autocorrelation matrices of the channel and the noise are given by (11) and (13) at the top of the next page.

$$\mathcal{E}\{\underline{\mathbf{H}\mathbf{H}}^H\} = \mathcal{E}\left\{\begin{bmatrix}\mathbf{H}_n\\ \vdots \\ \mathbf{H}_{n+N_{wind}-1}\end{bmatrix}\begin{bmatrix}\mathbf{H}_n^* & \cdots & \mathbf{H}_{n+N_{wind}-1}^*\end{bmatrix}\right\} = \begin{bmatrix}\Gamma(0) & \Gamma(1) & \cdots & \Gamma(N_{wind}-1)\\ \Gamma(-1) & \Gamma(0) & \cdots & \Gamma(N_{wind}-2)\\ \vdots & \vdots & \ddots & \vdots \\ \Gamma(1-N_{wind}) & \Gamma(2-N_{wind}) & \cdots & \Gamma(0)\end{bmatrix}, \quad (11)$$

where

$$\Gamma(\kappa) \triangleq diag\left\{P_s\varphi_{sd}^t[\kappa],\ P_s f_{AM_{r_1}}^2\varphi_{sr_1}^t[\kappa]\varphi_{r_1d}^t[\kappa],\cdots,\ P_s f_{AM_{r_{U-1}}}^2\varphi_{sr_{U-1}}^t[\kappa]\varphi_{r_{U-1}d}^t[\kappa]\right\}. \quad (12)$$

$$\mathcal{E}\{\underline{\mathbf{W}\mathbf{W}}^H\} = \mathbf{I}_{N_{wind}} \otimes diag\left\{N_0,\ (\sigma_{r_1d}^2 f_{AM_{r_1}}^2+1)N_0,\cdots,(\sigma_{r_{U-1}d}^2 f_{AM_{r_{U-1}}}+1)N_0\right\}. \quad (13)$$

With the aid of Bayes' theorem [8], the decision metric of the ML-MSDD can be expressed as:

$$\underline{\hat{\mathbf{S}}_{ML}} = \arg\min_{\underline{\mathbf{S}}\in\mathcal{C}^{N_{wind}}} Tr\{\underline{\mathbf{Y}}^H\underline{\Psi}^{-1}\underline{\mathbf{Y}}\}, \quad (14)$$

where $\mathcal{C}$ is the user-cooperation based signal constellation set. Note that due to the use of the Gaussian approximation, (14) becomes suboptimal in the context of the DAF-aided user-cooperation aided system of Fig. 1.

B. Multiple-Symbol Differential Sphere Detection Design

The equivalent user-cooperation based transmitted signal matrix $\underline{\mathbf{S}_d}$ as constructed in (4) for the DAF-aided cooperative system is a unitary matrix, hence we have:

$$\underline{\mathbf{S}_d}^{-1} = \underline{\mathbf{S}_d}^H. \quad (15)$$

Additionally, since the noise contributions imposed at the relay and destination nodes are both temporally and spatially uncorrelated, thus the autocorrelation $\mathcal{E}\{\underline{\mathbf{W}\mathbf{W}}^H\}$ is a diagonal matrix. Hence we can reformulate (10) as:

$$\underline{\Psi} = \underline{\mathbf{S}_d}(\mathcal{E}\{\underline{\mathbf{H}\mathbf{H}}^H\} + \mathcal{E}\{\underline{\mathbf{W}\mathbf{W}}^H\})\underline{\mathbf{S}_d}^H, \quad (16)$$

$$= \underline{\mathbf{S}_d}\mathbf{C}\underline{\mathbf{S}_d}^H, \quad (17)$$

where we have

$$\mathbf{C} \triangleq \mathcal{E}\{\underline{\mathbf{H}\mathbf{H}}^H\} + \mathcal{E}\{\underline{\mathbf{W}\mathbf{W}}^H\}, \quad (18)$$

which is defined as the $(UN_{wind} \times UN_{wind})$-element *channel-noise autocorrelation* matrix. Then, the metric of the ML-MSDD can be reformulated by substituting (17) characterizing Ψ in (14) and using (15), thus we arrive at:

$$\underline{\hat{\mathbf{S}}_{ML}} = \arg\min_{\underline{\mathbf{S}}\in\mathcal{C}^{N_{wind}}} Tr\{\underline{\mathbf{Y}}^H(\underline{\mathbf{S}_d}\mathbf{C}\underline{\mathbf{S}_d}^H)^{-1}\underline{\mathbf{Y}}\}, \quad (19)$$

$$= \arg\min_{\underline{\mathbf{S}}\in\mathcal{C}^{N_{wind}}} Tr\{\underline{\mathbf{Y}}^H\underline{\mathbf{S}_d}\mathbf{C}^{-1}\underline{\mathbf{S}_d}^H\underline{\mathbf{Y}}\}. \quad (20)$$

In the following discourse, we will transform the ML-MSDD metric of (14) to a *shortest-vector* problem by assuming the employment of a single antenna for each terminal for the sake of simplicity, which in turn can be efficiently solved by the multi-dimensional tree search aided sphere detector (SD) proposed in [9]. First of all, let us now introduce a transformation operator $T_d(\cdot)$ for a single-column matrix $\underline{\mathbf{B}}$ constituted by N_{wind} number of $(U \times 1)$-element sub-matrices $\mathbf{B}_n, (n = 0, 1, \cdots, N_{wind} - 1)$, which can be expressed as:

$$\underline{\mathbf{B}} = [\mathbf{B}_0^T \ \mathbf{B}_1^T \ \cdots \ \mathbf{B}_{N_{wind}-1}^T]^T. \tag{21}$$

When the transformation operation $T_d(\cdot)$ is applied to $\underline{\mathbf{B}}$, we arrive at:

$$T_d(\underline{\mathbf{B}}) = \begin{bmatrix} \boldsymbol{\Upsilon}_0 & 0 & \cdots & 0 \\ 0 & \boldsymbol{\Upsilon}_1 & \cdots & 0 \\ \vdots & \vdots & \ddots & \vdots \\ 0 & 0 & \cdots & \boldsymbol{\Upsilon}_{N_{wind}-1} \end{bmatrix}, \tag{22}$$

where $\boldsymbol{\Upsilon}_n \triangleq \mathbf{I}_{U\times U} \otimes \mathbf{B}_n^T$, which has $(U \times U^2)$ elements. Consequently, the resultant matrix $T_d(\underline{\mathbf{B}})$ constains N_{wind} block matrices $\boldsymbol{\Upsilon}_n$ $(n = 1, 2, \cdots, N_{wind})$ along the main diagonal of (22), leading to $(UN_{wind} \times U^2 N_{wind})$ elements.

Consequently, given the operator $T_d(\cdot)$ defined in (22), we can reformulate the ML-MSDD metric of (20) as:

$$\begin{aligned} \underline{\hat{\mathbf{S}}_{ML}} &= \arg \min_{\mathbf{s}\leftrightarrow\underline{\mathbf{S}}\in\mathcal{C}^{N_{wind}}} Tr\{(T_d(\underline{\mathbf{Y}})\mathbf{s}^*)^H \mathbf{C}^{-1} T_d(\underline{\mathbf{Y}})\mathbf{s}^*\}, \\ &= \arg \min_{\mathbf{s}\leftrightarrow\underline{\mathbf{S}}\in\mathcal{C}^{N_{wind}}} Tr\{\mathbf{s}^T T_d(\underline{\mathbf{Y}})^H \mathbf{C}^{-1} T_d(\underline{\mathbf{Y}})\mathbf{s}^*\}, \end{aligned} \tag{23}$$

where

$$\mathbf{s} = [\mathrm{vec}(\mathbf{S}_\mathrm{n})^\mathrm{T} \ \mathrm{vec}(\mathbf{S}_{\mathrm{n}+1})^\mathrm{T} \cdots \ \mathrm{vec}(\mathbf{S}_{\mathrm{n}+\mathrm{N}_{\mathrm{wind}}-1})^\mathrm{T}]^\mathrm{T}. \tag{24}$$

Then, by further constructing a $(UN_{wind} \times U^2 N_{wind})$-element upper-triangular block matrix $\mathbf{U}$ as:

$$\mathbf{U} \triangleq (\mathbf{F} T_d(\underline{\mathbf{Y}}))^*, \tag{25}$$

where the $(UN_{wind} \times UN_{wind})$-element upper-triangular matrix $\mathbf{F}$, which satisfies $\mathbf{F}^H\mathbf{F} = \mathbf{C}^{-1}$ with the aid of Cholesky factorization, we finally arrive at:

$$\underline{\hat{\mathbf{S}}_{ML}} = \arg \min_{\mathbf{s}\leftrightarrow\underline{\mathbf{S}}\in\mathcal{C}^{N_{wind}}} ||\mathbf{U}\mathbf{s}||^2, \tag{26}$$

which completes the process of transforming the ML-MSDD metric of (14) to a *shortest-vector* problem. Due to lack of space, the well-established SD algorithm will not be detailed here, please refer to [9, 10].

IV. Simulation Results and Discussion

It is well-understood that the DPSK-aided non-cooperative system employing the CDD suffers from a 3 dB performance loss in comparison to its coherent-modulation-assisted counterpart in the context of slow fading channels, i.e. when experiencing a normalized Doppler frequency of $f_d = 0.001$, as seen in Fig. 3, where an identical normalized Doppler frequency is assumed to be exhibited by each link of the user-cooperation aided system. Thanks to the DAF scheme, the two-user cooperation-aided system, which attains the maximum achievable diversity order of two, is capable of outperforming both of the above-mentioned non-cooperative systems without requiring high-complexity channel estimation. However, the time-selectivity of the fast-fading channel may severely impair the achievable performance of the CDD at the destination node. More explicitly, observe in Fig. 3 that the BER curve of the two-user cooperation-aided system levels out just below 10^{-3}, as P/N_0 increases. For the sake of exploiting the correlation between the channel-induced phase-rotation experienced by multiple consecutive transmitted DPSK symbols and hence to reduce the detrimental impact imposed by the time-selective channel on the DAF-aided system considered, the proposed MSDSD using $N_{wind} = 11$ was employed by the destination node at the expense of a higher computational complexity. Remarkably, the error floor encountered by the system employing the CDD in fast-fading channels was essentially eliminated. For example, the BER curve corresponding to the MSDSD-aided cooperative system obtained for $f_d = 0.03$ coincides with that of its CDD-aided counterpart, which was recorded for a relatively slowly-fading channel associated with $f_d = 0.001$, resulting in a performance gain of more than 10 dB, at a target BER of 10^{-3}. Furthermore, the former system operating in a fast fading channel having $f_d = 0.01$ is capable of outperforming the latter, even if the latter is operating in a slow fading channel having $f_d = 0.001$.

	$f_{d,sd}$	$f_{d,sr}$	$f_{d,rd}$
Scenario I	0.03	0.03	0.001
Scenario II	0.001	0.03	0.03
Scenario III	0.03	0.001	0.03

TABLE I

Doppler frequency allocation of three different scenarios.

In Fig. 4 the BER curves corresponding to the three different scenarios of Table I are bounded by the two dashed-dotted BER curves having no legends, which were obtained by assuming an identical normalized Doppler

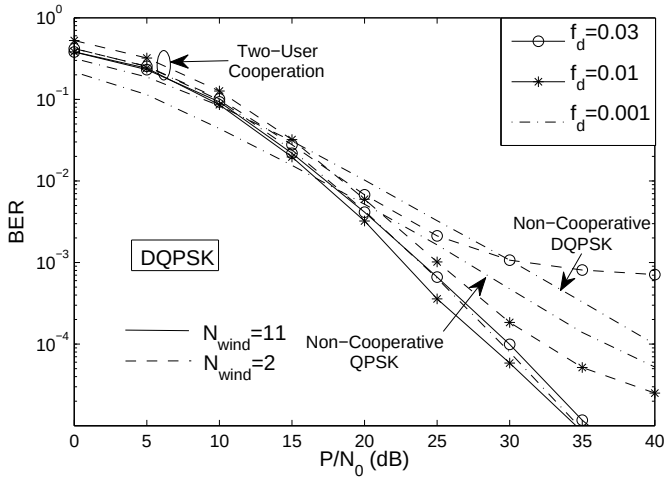

Fig. 3. BER performance improvement achieved by the MSDSD employing $N_{wind} = 11$ for the DAF-aided DQPSK-modulated two-user cooperative system in a time-selective Rayleigh fading channel.

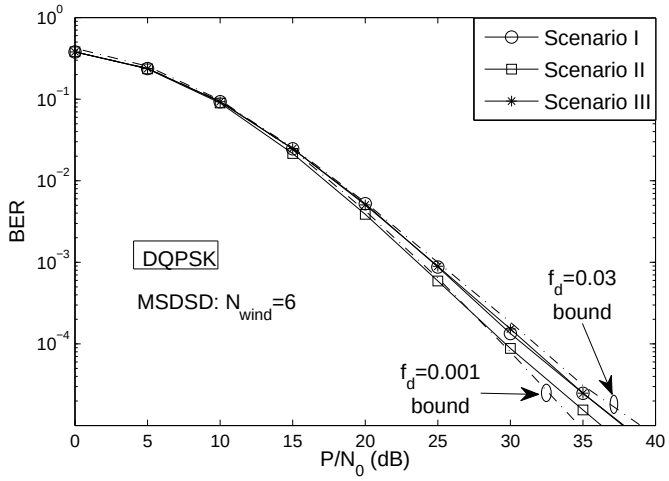

Fig. 4. The impact of the relative mobility among the source, relay and destination nodes on the BER performance of the DAF-aided DQPSK-modulated two-user cooperative system in Rayleigh fading channels.

frequency of $f_d = 0.03$ and $f_d = 0.001$ for each link in the user-cooperation aided system, respectively. In all the three situations, only one of the three nodes in the two-user cooperation-aided system is supposed to move relative to the other two nodes at a speed resulting in a normalized Doppler frequency of 0.03, while the latter two remain immobile relative to each other, yielding a normalized Doppler frequency of 0.001. Since the channel quality of the direct link characterized in terms of its grade of time-selectivity predetermines the achievable performance of the

DAF-aided user-cooperation system employing the MSDSD, it is observed in Fig. 4 that the system is capable of attaining a better BER performance in Scenario II ($f_{d,sd} = 0.001$) than in the other two scenarios ($f_{d,sd} = 0.03$). On the other hand, the MSDSD-aided system exhibits a similar performance in Scenario I and Scenario III, since the source-relay and relay-destination links are symmetric and thus they are exchangable in the context of the DAF scheme, as observed in (12).

V. Conclusion

A MSDSD scheme was proposed for mitigating the error floor encountered by the DAF-aided user-cooperation aided system in time-selective channels, leading to a significant performance gain over the system using the CDD. For example, given a target BER of 10^{-3}, a performance gain of about 10 dB can be attained by the proposed MSDSD employing $N_{cand} = 11$ for a DQPSK modulated cooperative two-user system in a relatively fast-fading channel having a normalized Doppler frequency of 0.03.

References

[1] G. J. Foschini and M. J. Gans, "On limits of wireless communications in a fading environment when using multiple antennas," *Wireless Personal Communications*, vol. 6, pp. 311–335, Mar. 1998.

[2] J. N. Laneman, D. N. C. Tse, and G. W. Wornell, "Cooperative diversity in wireless networks: Efficient protocols and outage behavior," *IEEE Transaction on Information Theory*, vol. 50, pp. 3062–3080, Dec. 2004.

[3] K. G. Seddik, A. K. Sadek, W. Su, and K. J. R. Liu, "Outage analysis and optimal power allocation for multinode relay networks," *IEEE Signal Processing Letters*, vol. 14, pp. 377–380, June 2007.

[4] T. Himsoon, W. Su, and K. J. R. Liu, "Differential transmission for amplify-and-forward cooperative communications," *IEEE Signal Processing Letters*, vol. 12, pp. 597–600, Sept. 2005.

[5] L. Lampe, R. Schober, V. Pauli, and C. Windpassinger, "Multiple-symbol differential sphere decoding," *IEEE Transactions on Communications*, vol. 12, pp. 1981–1985, Dec. 2005.

[6] V. Pauli and L. Lampe, "Multiple-symbol differential sphere decoding for unitary space-time modulation," *IEEE Global Telecommunications Conference*, vol. 3, p. 6, Nov. 2005.

[7] R.-R. Chen, R. Koetter, and U. Madhow, "Multiple-antenna differential lattice decoding," *Conference on Information Sciences and Systems*, 2003, http://citeseerx.ist.psu.edu/viewdoc/summary?doi=10.1.1.12.6561.

[8] L. Hanzo, M. Munster, B. J. Choi, and T. Keller, *OFDM and MC-CDMA for Broadband Multi-User Communications, WLANs and Broadcasting*. IEEE Press, 2003.

[9] L. Wang, O. Alamri, and L. Hanzo, "Sphere packing modulation in the SDMA uplink using K-best sphere detection," *IEEE Signal Processing Letters*, vol. 16, pp. 291–294, Apr. 2009.

[10] M. O. Damen, H. E. Gamal, and G. Caire, "On maximum-likelihood detection and the search for the closest lattice point," *IEEE Transactions on Information Theory*, vol. 49, pp. 2389–2402, Oct. 2003.